

Fig. 4. Frequency characteristics at different supply voltages. Triangles mark data recorded for operation at  $-4.5$  V, open circle at  $-5.0$  V, and closed circle at  $-5.5$  V.

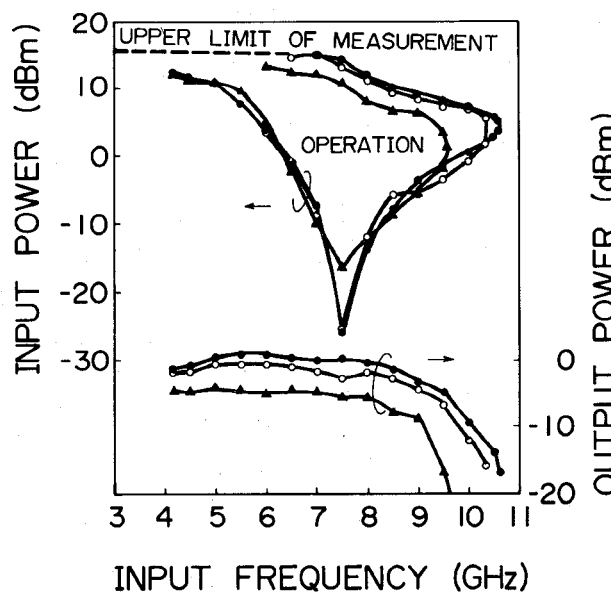


Fig. 5. Frequency characteristics at different supply voltages. Triangles mark data recorded for operation at  $-6.3$  V, open circle at  $-7.0$  V, and closed circle at  $-7.7$  V.

#### IV. SUMMARY

New 2.0–8.0 GHz and 6.0–10.5 GHz dynamic frequency dividers have been developed. The divider was constructed with a double-loop connected pair of differential amplifiers. The frequency divider was operated from one voltage supply at  $-5$  V, or  $-7$  V with  $\pm 10$  percent voltage supply fluctuation. This divider overcomes the weak points of conventional dynamic dividers, which need two voltage supplies and precise supply voltage control. This divider operates at a 50 percent higher frequency than static dividers.

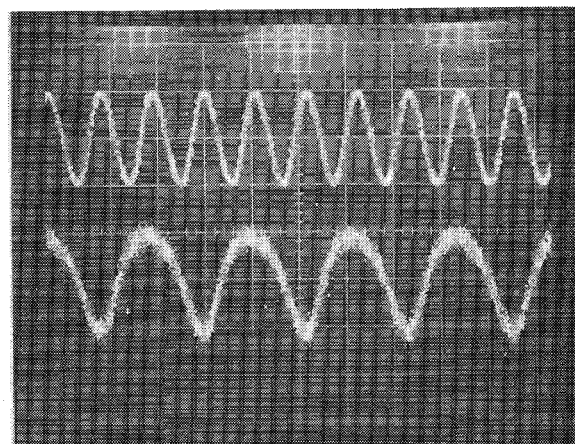


Fig. 6. Input and output waveforms of the frequency divider. Top: input waveform. Bottom: output waveform. 20 dB attenuator inserted between D.U.T. and sampling oscillator. Vertical axis: 50 mV/div. (input); 10 mV/div. (output). Horizontal axis: 100 ps/div.

#### ACKNOWLEDGMENT

The authors would like to thank Messrs. Onodera, Shibata, Nakayama, Ishiguro, and Sakuma for their technical support and discussions. They would also like to thank Dr. Fukuta, Dr. Nishi, and Messers. Izumi, Ashida, and Yamada, who encouraged us in this study.

#### REFERENCES

- [1] M. Rocchi, and B. Gabillard, "GaAs digital dynamic IC's for applications up to 10 GHz," *IEEE J. Solid-State Circuits*, vol. SC-18, no. 3, pp. 369–376, 1983.
- [2] M. Iwakuni, M. Shigaki, S. Yokogawa, and K. Sakuma, "6.5 GHz dynamic frequency divider with oscillator," in *National Conf. Rec. IECE Japan*, vol. 1, 1986, p. 110.
- [3] K. Osafume and K. Ohwada, "An ultra-high-speed GaAs prescaler using a dynamic frequency divider," *IEEE Trans. Microwave Theory Tech.*, vol. MTT-35, pp. 9–13, 1987.
- [4] S. Asai, N. Goto, M. Kanamori, Y. Tanaka, and T. Furutsuka, "A high performance LDD GaAs MESFET with a refractory metal gate," in *Proc. 18th Conf. Solid State Devices Mater.*, 1986, pp. 383–380.

#### Properties of Shielded Cylindrical Quasi- $TE_{0nm}$ -Mode Dielectric Resonators

JERZY KRUPKA

**Abstract**—Comparison of the Rayleigh–Ritz method and the mode-matching method for computations of quasi- $TE_{0nm}$ -mode frequencies and unloaded  $Q$  factors of shielded dielectric resonators is presented. Rigorous bounds for the true quasi- $TE_{0nm}$ -mode frequencies are assessed. Influence of various parameters on the resonant frequencies, unloaded  $Q$  factors, and the temperature coefficients of the resonant frequency is demonstrated for many shielded dielectric resonator structures. Different approaches to unloaded  $Q$  factor computations are discussed and numerically compared.

Manuscript received May 14, 1987; revised October 28, 1987.

The author is with the Instytut Mikroelektroniki i Optoelektroniki, Politechnika Warszawska, 00-662 Warszawa, Poland.

IEEE Log Number 8719201.

## I. INTRODUCTION

During the last two decades many rigorous methods of analyzing dielectric resonators (DR's) have been developed, such as the mode-matching method [1]–[4], the finite element method [5], [6], the finite difference method [7], and the Rayleigh–Ritz method [8], [9]. However, studies comparing various methods have not appeared in the literature yet.

The purpose of this paper is twofold. The first is to compare the results of computations of the resonant frequencies and unloaded  $Q$  factors  $Q_u$  of quasi-TE<sub>0nm</sub>-mode DR's using the mode-matching and Rayleigh–Ritz techniques. The second is to present numerical results illustrating the influence of various parameters on the resonant frequencies,  $Q_u$  factors, and the temperature coefficients for many shielded quasi-TE<sub>0nm</sub>-mode DR's. The mode-matching and Rayleigh–Ritz methods have been chosen for analysis, since they provide lower and upper bounds for the true resonant frequencies of lossless quasi-TE<sub>0nm</sub>-mode resonant systems. Therefore in such cases the accuracy of computations can be rigorously assessed.

## II. THEORY

### A. Methods of Unloaded $Q$ -Factor Computations

Applications of the mode-matching method and the Rayleigh–Ritz method for computation of the resonant frequencies and unloaded  $Q_u$  factors of cylindrical quasi-TE<sub>0nm</sub>-mode DR's have been described in the literature, e.g. [1]–[4], [8], [9]. Since for  $Q_u$ -factor computations we have certain alternative approaches, we consider this problem in detail. The resonant system we are concerned with is sketched in Fig. 1. The most general approach of  $Q_u$ -factor computation is a conception of the complex frequency which is introduced in Maxwell's equations and then in the characteristic equation. This method makes it possible, in the source-free region of the resonant system, to determine simultaneously the resonant frequencies ( $f = \text{Re}(\omega)/2\pi$ ) and  $Q_u$  factors ( $Q_u = \text{Re}(\omega)/2\text{Im}(\omega)$ ) of the system. All losses can be simultaneously considered. Dielectric losses and conductor losses can be represented in the same manner as imaginary parts of permittivities [4]. Since this method is complicated for low-loss systems (nonradiating systems whose frequencies do not depend significantly on losses), other methods of  $Q_u$ -factor computation are commonly used. Lossless systems containing only perfect conductors and dielectrics are considered as the first step in these methods, and the resonant frequencies and the field distributions of the systems are found. Then, as the second step, the  $Q_u$  factor is computed using the definition:  $Q_u = \omega$  (the energy stored)/(the average power dissipated), assuming that for lossy resonant systems the electromagnetic field distributions remain the same as for the lossless systems. Then we can express the reciprocal of the  $Q_u$  factor as follows [10]:

$$Q_u^{-1} = Q_d^{-1} + Q_c^{-1} \quad (1)$$

$$Q_d^{-1} = \sum_{i=1}^I p_{ei} \tan \delta_i \quad (2)$$

$$Q_c = A/R_s \quad (3)$$

$$p_{ei} = W_{ei}/W_e = \left( \int_{V_i} \epsilon_i |\vec{E}_i|^2 dv \right) / \left( \sum_{i=1}^I \int_{V_i} \epsilon_i |\vec{E}_i|^2 dv \right) \quad (4)$$

$$A = \left( \omega \sum_{i=1}^I \int_{V_i} \epsilon_i |\vec{E}_i|^2 dv \right) / \left( \int_S |\vec{H}_t|^2 ds \right) \quad (5)$$

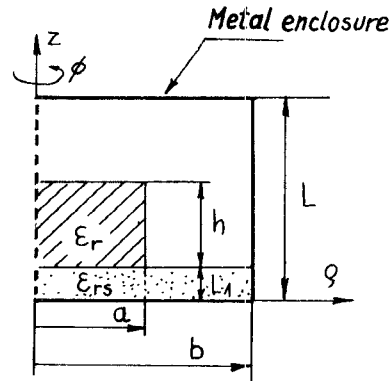


Fig. 1. Cylindrical dielectric resonator on a substrate in a metal shield.

where

- $I$  number of subregions ( $V_i$ ) of the resonant structure having different loss tangent ( $\tan \delta_i$ ) values,
- $S$  surface of the metal shield,
- $R_s$  surface resistance of the metal shield,
- $\vec{E}, \vec{H}$  electric and magnetic fields of the lossless resonant system.

The coefficients  $p_{ei}$  (called the electric energy filling factors) and  $A$ , which appear in the above equations, depend only on permittivities and on relative dimensions of the system, so the results for  $p_{ei}$  and  $A$  are representative for resonators operating at any frequency value. There are two methods for evaluation of the integral ratios appearing in (4) and (5). In the first the electromagnetic fields are substituted into (4) and (5) and integrations are performed directly. In the second, perturbation theory is used. Cavity material perturbation theory is used for  $p_{ei}$  computations [3] and cavity wall perturbation theory (incremental frequency rule) [11] for  $A$ -factor computations. In the last case, the theory is valid only for resonant systems whose normal components of the electric field vanish on the metal shield. We can also mix different formalisms. For example, depending on dielectric losses, the  $Q_d$  factor can be computed using complex frequency formalism, while the  $Q_c$  factor, depending on conductor losses, can be computed by means of perturbation theory.

### B. Methods of Temperature Coefficient Computation

Due to temperature variations, each material expands with its own temperature expansion coefficient and each dielectric constant changes its value with its own temperature coefficient of dielectric constant. When we evaluate all the differentials for the resonant system shown in Fig. 1, we obtain the following formula for the relative change of frequency due to temperature [10]:

$$\tau_f = C_L \alpha_L + C_h \alpha_h + C_{L1} \alpha_{L1} + C_{\epsilon_r} \tau_{\epsilon_r} + C_{\epsilon_{rs}} \tau_{\epsilon_{rs}} \quad (6)$$

where the  $\alpha$ 's are the temperature expansion coefficients and the  $\tau$ 's are the temperature coefficients of frequency or dielectric constants. The  $C$  coefficients can be evaluated numerically as

$$C_x = \frac{\partial f}{f} / \frac{\partial x}{x} = \frac{\partial f}{\partial x} \cdot \frac{x}{f} \quad (7)$$

where  $x$  denotes any parameter (dimension or permittivity).

Usually the metal shield is made of homogeneous metal and the dielectric of the DR is isotropic so  $\alpha_L = \alpha_h = \alpha_m$  and  $\alpha_a =$

$= \alpha_d$ . Then we can rewrite (6) as follows:

$$\tau_f = C_m \alpha_m + C_d \alpha_d + C_{L1} \alpha_{L1} + C_{er} \tau_{er} + C_{ers} \tau_{ers} \quad (8)$$

where

$$C_d = C_a + C_h$$

$$C_m = C_b + C_L.$$

It is well known that if all dimensions of a resonant system are increased by a certain factor, the resonant frequency of the system decreases by the same factor. As a result, the coefficients  $C_m$ ,  $C_d$ , and  $C_{L1}$  satisfy the following equation:

$$C_m + C_d + C_{L1} = -1. \quad (9)$$

If two coefficients are known (one if  $L_1 = 0$ ), the remaining one can be calculated from (9). The coefficients  $C_{er}$  and  $C_{ers}$  are related to the electric energy filling factors. It can be proved from the material perturbation theorem that [3]

$$|C_{er}| = (2W_e/W_{er})^{-1} = p_{er}/2. \quad (10)$$

The coefficients  $C_L$ ,  $C_b$ , and  $C_{L1}$  are related to the  $A$  factor. We can prove from the cavity wall perturbation theorem that

$$A = \omega \mu_0 L / [2(|C_L| + |C_{L1}|L/L_1 + |C_b|L/b)] \quad (11)$$

(for  $L_1 = 0$ ,  $|C_b|L/h$  instead of  $|C_{L1}|L/L_1$  must be substituted in (11)).

### III. RESULTS OF COMPUTATIONS

Most numerical results are presented in general form independent of absolute dimensions, physical constants, and loss parameters. Since for cylindrical rod DR's, the TE<sub>011</sub>-mode frequency, denoted in this paper by  $f_{rod}$ , is usually known, we have reduced the TE<sub>018</sub> (quasi-TE<sub>011</sub>) frequencies with respect to  $f_{rod}$  values. Higher order quasi-TE<sub>0nm</sub>-mode frequencies have been reduced with respect to the velocity of light. For cavity-type resonant systems the classical Rayleigh-Ritz method (R) has been used with empty cavity TE<sub>0nm</sub>-mode basis (100 basis functions), while for open-type systems the modified Rayleigh-Ritz method (MR) [9] has been used with rod resonator TE<sub>0nm</sub>-mode basis (25 basis functions). The radial mode-matching method (M-M) has been used with nine functions in each of the two complementary regions. For these numbers of basis functions all methods require approximately the same time for computation (approximately 10 seconds on a CDC 6600 computer per frequency value). The computer program for the modified Rayleigh-Ritz method has been written in complex version, while two others are in real versions. Some of the results have been obtained by a complex version of the mode-matching method (the computer program has been written by Sz. Maj).

We denote different methods of  $A$  and  $p_e$  factor computations as follows: C for the complex frequency method, I for the incremental frequency (perturbation) method, and D for the method using direct integration of the electromagnetic fields.

Table I gives results of computations for a cavity-type resonator having  $\epsilon_r = 10$ ,  $a/h = 1$ ,  $b/L = 1$ , and  $L_1 = 0$ . It is seen that the frequency values computed by the Rayleigh-Ritz method and by the mode-matching method agree to within 0.15 percent for any  $p = h/L$  value. The maximum discrepancy appears for  $p = 0.25$ . Also,  $A$ -factor values agree to within 0.35 percent if the incremental frequency rule is used in both methods. If the direct integration method (D) is used, differences in  $A$ -factor values obtained by the mode-matching and Rayleigh-Ritz methods are somewhat greater. For interior modes (modes whose energy is predominantly concentrated in the dielectric) the electric energy

TABLE I  
THE COMPUTED VALUES OF NORMALIZED TE<sub>018</sub>-MODE  
FREQUENCIES  $f/f_{rod}$ , THE ELECTRIC ENERGY RATIO  $p_e^{-1}$ ,  $A$ , AND  
 $C_m$  COEFFICIENTS VERSUS  $h/L$  FOR A DR SITUATED IN A  
CYLINDRICAL CAVITY

$h/L$	$f/f_{rod}$	$p_e^{-1}$			$A$			$C_m$
		M-M	R	M-M(I)	R(I)	R(D)	M-M(I)	
0.00	0.0000	0.0000	$\infty$	$\infty$	$\infty$	665.7	665.7	665.7 -1.000
0.15	0.5390	0.5390	364.37	380.20	380.80	660.8	661.2	660.8 -0.994
0.20	0.7416	0.7418	14.12	14.76	14.80	623.3	624.4	624.5 -0.885
0.25	0.8030	0.8042	1.443	1.442	1.443	519.1	519.3	529.8 -0.181
0.30	0.8181	0.8188	1.171	1.171	1.171	514.7	516.5	501.8 -0.065
0.35	0.8253	0.8257	1.118	1.118	1.118	516.5	517.0	516.8 -0.054
0.40	0.8312	0.8315	1.092	1.092	1.092	515.3	515.6	522.1 -0.059
0.45	0.8377	0.8379	1.074	1.074	1.074	510.8	511.8	505.4 -0.074
0.50	0.8452	0.8454	1.060	1.060	1.060	501.9	502.3	502.0 -0.098
0.60	0.8660	0.8661	1.038	1.038	1.038	464.1	464.7	460.5 -0.179
0.70	0.8989	0.8989	1.021	1.021	1.024	395.8	396.6	400.8 -0.321
0.80	0.9510	0.9510	1.008	1.008	1.008	311.4	312.0	308.0 -0.543
0.90	1.0304	1.0304	1.001	1.001	1.001	240.0	240.5	241.5 -0.829
1.00	1.1362	1.1362	1.000	1.000	1.000	210.1	210.1	210.1 -1.000

$\epsilon_r = 10$ ,  $a/h = b/L$ ,  $L_1 = 0$ . M-M denotes the mode-matching method results with  $N = 9$ . R denotes the Rayleigh-Ritz method results with  $N = 100$ .

TABLE II  
THE COMPUTED VALUES OF NORMALIZED QUASI-TE<sub>0nm</sub>-MODE  
FREQUENCIES  $\omega L/c$  VERSUS THE NUMBER OF BASIS FUNCTIONS  $N$   
FOR THE MODE-MATCHING METHOD

N	$\frac{\omega}{c} L$					
	TE <sub>011</sub>	TE <sub>012</sub>	TE <sub>021</sub>	TE <sub>022</sub>	TE <sub>043</sub>	TE <sub>031</sub>
1	4.07981	—	—	—	—	—
2	4.32412	5.15487	—	—	—	—
3	4.40270	5.15801	—	749754	7.90860	8.19561
4	4.42289	5.16582	715565	745886	7.91231	8.21483
5	4.42405	5.16837	7.23677	746290	7.90435	8.21437
6	4.42393	5.16866	7.27404	746977	7.99954	8.21784
7	4.42488	5.16866	7.28842	747364	7.99744	8.22207
8	4.42560	5.16869	7.29109	747431	7.89711	8.22418
9	4.42575	5.16872	7.29072	747419	7.89722	8.22449
R	4.43245	5.17032	7.31309	7.49125	7.94563	8.25259

The DR is situated in a cylindrical cavity.  $\epsilon_r = 10$ ,  $a/h = b/L = 1.00$ ,  $h/L = 0.25$ . M-M and R have the same meanings as in Table I

filling factor values, computed by both methods, agree to within 0.1 percent. Greater discrepancy occurs for exterior modes.

Table II gives results of computations of higher order quasi-TE<sub>0nm</sub>-mode frequencies for the same resonant system and  $p = 0.25$ . Convergence of the mode-matching method is investigated versus number of basis functions ( $N$ ). In the last row of Table II results obtained by the Rayleigh-Ritz method are shown. It is seen that the discrepancy between frequency values obtained by these two methods is not greater than 0.6 percent for the first six modes. Results of higher order frequencies and the electric energy filling factor computations versus  $p = h/L$  values are shown in Fig. 2. Computations were performed by the Rayleigh-Ritz method. We can observe in Fig. 2 that the frequency curves show the intervals of plateaus alternating with intervals of steep slope. In the intervals of steep slope the  $p_e$  values are close to unity and the modes are of the interior type, while in the intervals of plateaus the modes become of the exterior type. This phenomenon has already been reported in [1] and [12].

Results of computations for the resonant system having  $\epsilon_r = 35$ ,  $a/h = 1$ ,  $b/L = 1$ , and  $L_1 = 0$  are presented in Table III. For  $p \geq 0.25$  results of computations agree very well (similarly as for  $\epsilon_r = 10$ ). For  $p < 0.20$ , the differences increase. This is understood, since for small  $p$  values and high  $\epsilon_r$  values the convergence of the classical Rayleigh-Ritz method becomes poor [8]. We can observe that when the DR is placed at the cavity bottom,

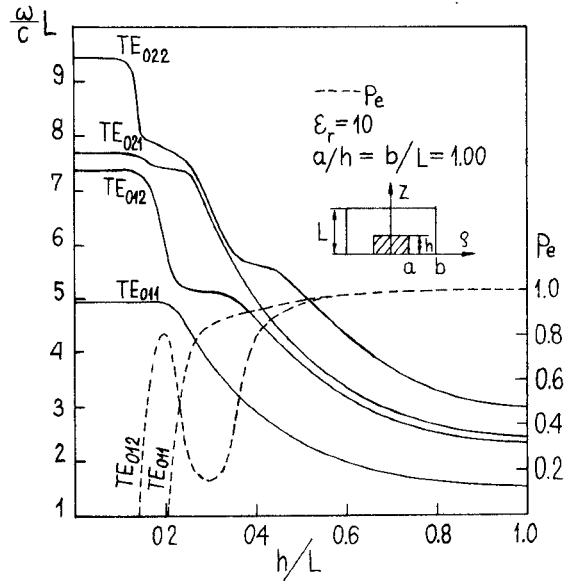


Fig. 2. The lowest quasi- $TE_{0nm}$ -mode normalized frequencies ( $\omega L/c$ ) and the electric energy filling factor values  $p_e$  versus the  $h/L$  ratio for a cylindrical DR situated at the cavity bottom.  $\epsilon_r = 10$ ,  $a/h = 1$ ,  $b/L = 1$ . The results have been obtained by means of the Rayleigh-Ritz method with  $N = 100$ .

TABLE III  
THE COMPUTED VALUES OF NORMALIZED  $TE_{018}$ -MODE  
FREQUENCIES  $f/f_{\text{rod}}$ , THE ELECTRIC ENERGY RATIO  $p_e^{-1}$ , A, AND  
 $C_m$  COEFFICIENTS VERSUS  $h/L$  FOR A DR SITUATED IN A  
CYLINDRICAL CAVITY

$h/L$	$f/f_{\text{rod}}$	$p_e^{-1}$			A			$C_m$
		M-M	R	M-M(I)	R(I)	R(D)	M-M(I)	
0.00	0.0000	0.0000	$\infty$	$\infty$	$\infty$	$\infty$	665.7	-1.000
0.10	0.6692	0.6692	659.2	1410.	1413.	661.0	663.1	-0.998
0.125	0.8274	0.8332	2754	15.37	15.48	428.2	580.1	586.5
0.15	0.8416	0.8525	1.041	1.046	1.047	286.4	265.4	253.5
0.20	0.8429	0.8470	1.028	1.029	1.029	287.5	278.2	286.0
0.25	0.8440	0.8459	1.024	1.025	1.025	287.2	287.2	297.0
0.30	0.8449	0.8459	1.022	1.023	1.023	287.0	288.5	219.9
0.40	0.8487	0.8494	1.019	1.019	1.019	286.5	287.0	291.1
0.50	0.8567	0.8568	1.013	1.014	1.014	279.6	280.2	279.6
0.60	0.8722	0.8723	1.010	1.010	1.010	259.0	259.8	257.1
0.70	0.9006	0.9006	1.006	1.006	1.006	219.5	220.8	223.2
0.80	0.9487	0.9487	1.003	1.003	1.003	170.4	171.5	169.0
0.90	1.0255	1.0255	1.000	1.000	1.000	129.1	129.8	130.2
1.00	1.1313	1.1313	1.000	1.000	1.000	112.5	112.5	112.5

$\epsilon_r = 35$ ,  $a/h = b/L = 1.00$ ,  $L_1 = 0$ . M-M and R have the same meanings as in Table I.

as was the case for the resonant systems considered so far,  $A$ -factor values are smaller than that of the empty cavity. If the DR is placed far from the cavity walls,  $A$ -factor values can be much higher, as is seen in Fig. 3, which presents results of computations for a DR situated centrally in a cylindrical cavity. The Rayleigh-Ritz method has been used for computations. Maximum  $A$ -factor values appear for cavity dimensions 5–6 times greater than the DR ones ( $p = 0.15$ – $0.20$ ). For these  $p$  values the  $TE_{018}$  mode is interior since the electric energy filling factor values are high ( $p_e \geq 0.85$ ). For  $p$  values smaller than 0.15, the  $TE_{018}$  mode becomes exterior and  $A$ -factor values tend rapidly to the value characteristic of an empty  $TE_{011}$  mode cavity.

In Table IV results of computations for open-type nonradiating DR structures are presented. For all cases considered in Table IV, discrepancy between frequency values obtained by the modified Rayleigh-Ritz method and the mode-matching method is not greater than 0.15 percent.  $A$ -factor values agree to within

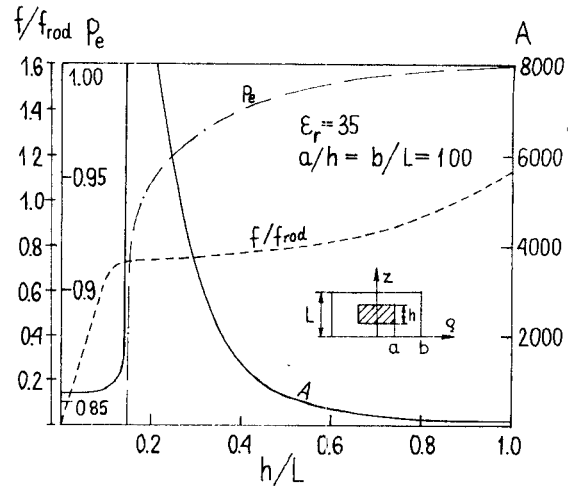


Fig. 3. Normalized  $TE_{018}$ -mode resonant frequency ( $f/f_{\text{rod}}$ ), the electric energy filling factor values  $p_e$ , and  $A$ -factor values versus the  $h/L$  ratio for a cylindrical DR situated centrally in cylindrical cavity.  $\epsilon_r = 35$ ,  $a/h = 1$ . The results have been obtained by means of the Rayleigh-Ritz method with  $N = 100$ .

TABLE IV  
THE COMPUTED VALUES OF NORMALIZED  $TE_{018}$ -MODE  
FREQUENCIES  $f/f_{\text{rod}}$ , THE ELECTRIC ENERGY RATIO  $p_e^{-1}$ , A, AND  
 $C_m$  COEFFICIENTS VERSUS  $L/\lambda_{\text{rod}}$  FOR AN OPEN-TYPE DR  
STRUCTURE

$a/h$	$L/\lambda_{\text{rod}}$	$f/f_{\text{rod}}$		$p_e^{-1}$			A			$C_m$
		M-M	R(C)	M-M(I)	R(I)	R(D)	M-M(I)	R(I)	R(D)	
0.25	0.2872	1.0000	1.0000	1.032	1.032	1.032	959.9	959.9	959.9	-0.178
	0.30	0.9927	0.9927	1.033	1.033	1.033	1077.7	1083.3	1074.6	-0.156
	0.35	0.9773	0.9774	1.042	1.042	1.042	1739.2	1744.7	1754.1	-0.059
	0.40	0.9717	0.9749	1.051	1.051	1.050	2022.4	2038.5	2058.3	-0.033
	0.45	0.9685	0.9689	1.061	1.061	1.059	2081.0	2096.6	2140.1	-0.024
	0.50	0.9660	0.9664	1.084	1.079	1.074	1954.0	2002.2	2137.9	-0.010
0.50	0.1711	1.0000	1.0000	1.042	1.042	1.042	294.4	294.4	294.4	-0.344
	0.20	0.9583	0.9583	1.045	1.045	1.046	445.7	447.4	444.7	-0.189
	0.25	0.9357	0.9357	1.022	1.022	1.022	660.1	664.7	667.4	-0.054
	0.30	0.9297	0.9298	1.026	1.026	1.027	722.0	723.2	730.5	-0.023
	0.35	0.9272	0.9276	1.030	1.029	1.029	737.3	739.2	737.2	-0.013
	0.40	0.9260	0.9264	1.033	1.032	1.032	741.0	743.5	760.3	-0.008
1.00	0.45	0.9251	0.9257	1.037	1.035	1.034	743.3	743.4	744.3	-0.009
	0.50	0.9240	0.9251	1.042	1.038	1.036	743.6	744.5	744.3	-0.014
	0.1177	1.0000	1.0000	1.004	1.004	1.004	119.6	119.6	119.6	-0.582
	0.15	0.8984	0.8984	1.006	1.006	1.007	189.7	190.3	190.7	-0.278
	0.20	0.8587	0.8588	1.013	1.013	1.014	262.6	262.8	262.8	-0.077
	0.25	0.8493	0.8494	1.018	1.018	1.018	280.5	280.7	280.4	-0.029
1.50	0.30	0.8461	0.8464	1.021	1.020	1.021	284.9	285.0	286.3	-0.015
	0.35	0.8445	0.8450	1.023	1.022	1.022	286.1	286.1	286.2	-0.010
	0.40	0.8436	0.8444	1.025	1.024	1.024	285.9	286.6	293.7	-0.006
	0.45	0.8431	0.8440	1.026	1.025	1.025	285.5	286.3	286.9	-0.004
	0.50	0.8427	0.8437	1.029	1.025	1.026	286.1	286.7	279.6	-0.004
	0.1023	1.0000	1.0000	1.002	1.002	1.002	84.0	84.0	84.0	-0.720
2.00	0.15	0.8314	0.8315	1.007	1.007	1.007	145.0	145.3	145.6	-0.243
	0.20	0.7968	0.7969	1.013	1.013	1.014	174.2	174.4	175.0	-0.082
	0.25	0.7871	0.7873	1.018	1.017	1.018	181.4	181.6	183.6	-0.035
	0.30	0.7834	0.7837	1.024	1.020	1.021	183.4	183.4	183.0	-0.019
	0.35	0.7817	0.7822	1.023	1.022	1.023	183.8	184.0	188.1	-0.011
	0.40	0.7808	0.7814	1.025	1.024	1.024	183.9	184.0	183.5	-0.007
3.00	0.45	0.7802	0.7810	1.027	1.025	1.025	184.3	184.3	180.3	-0.007
	0.50	0.7795	0.7807	1.029	1.026	1.026	185.0	183.8	184.1	-0.010

$\epsilon_r = 35$ ,  $L_1 = 0$ ,  $b = \infty$ . M-M denotes the mode-matching method results with  $N = 9$ . R denotes the modified Rayleigh-Ritz method with  $N = 25$ .

0.75 percent (except one value for  $a/h = 0.25$  and  $L/\lambda_{\text{rod}} = 0.50$ ) and  $p_e$  factor values agree to within 0.40 percent.

The results of normalized  $TE_{018}$ -mode frequency computations versus  $L/\lambda_{\text{rod}}$  values are presented in Fig. 4 together with experimental data for one DR structure. Experiments have been performed for a DR having  $h = 4.00$  mm,  $a = 3.42$  mm, and  $\epsilon_r = 34.2$ . We can note that systematic 0.01 mm error of DR dimensions for the DR used in experiments causes  $\sim 0.3$  percent

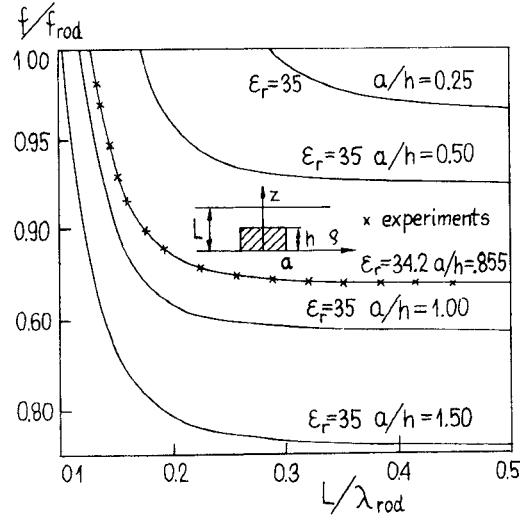


Fig. 4. Normalized  $TE_{018}$ -mode resonant frequencies ( $f/f_{\text{rod}}$ ) versus the  $L/\lambda_{\text{rod}}$  ratio for open-type DR's.  $\epsilon_r = 35$ ,  $b = \infty$ ,  $L_1 = 0$ . The results have been obtained by means of the modified Rayleigh-Ritz method with  $N = 25$ .

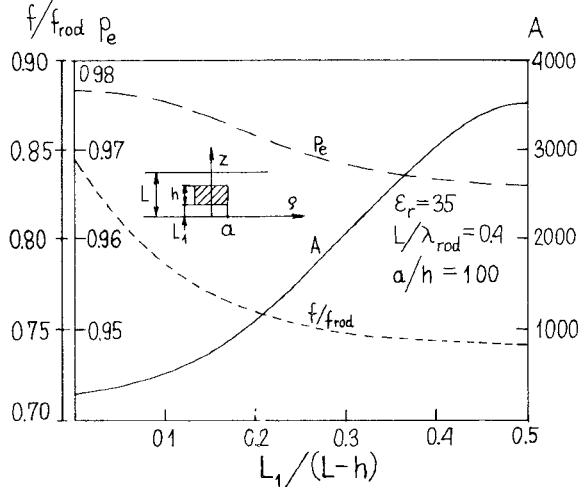


Fig. 5. Normalized  $TE_{018}$ -mode resonant frequency ( $f/f_{\text{rod}}$ ), the electric energy filling factor values  $p_e$ , and  $A$ -factor values versus the distance  $L_1/(L-h)$  between the dielectric resonator and the metal plate.  $\epsilon_r = 35$ ,  $L/\lambda_{\text{rod}} = 0.4$ ,  $a/h = 1$ . The results have been obtained by means of the modified Rayleigh-Ritz method with  $N = 25$ .

error in frequency value. Such error is greater than errors of computations.

In Fig. 5 we present the influence of the distance  $L_1$  between the dielectric resonator and the metal plate on the  $TE_{018}$ -mode frequency,  $p_e$ , and  $A$  factor values. The results have been obtained by the modified Rayleigh-Ritz method. As with cavity-type resonators, the  $A$  coefficient reaches a maximum for symmetric DR position. For the resonant system shown in Fig. 5, the maximum value of  $A$  is approximately equal to 3500. The value  $L/\lambda_{\text{rod}} = 0.4$  corresponds to the value of  $h/L = 0.294$ . For a centrally filled cavity with  $h/L = 0.3$  (Fig. 3) the value of  $A$  is only 3 percent less than for an open-type structure, so in this case conductor losses in the lateral surface of the cavity constitute only a small part of total conductor losses. The influence of the lateral surface on the resonant frequency, for the case considered here, is smaller than 0.5 percent. We find from the results shown in Table IV ( $L/\lambda_{\text{rod}} = 0.4$  and  $a/h = 1$ ) that for a similar case and  $L_1 = 0$  the influence of the lateral surface on  $A$ -factor values

TABLE V  
THE COMPUTED VALUES OF NORMALIZED  $TE_{018}$ -MODE  
FREQUENCIES  $f/f_{\text{rod}}$ , THE ELECTRIC ENERGY RATIO  $p_e^{-1}$ ,  $A$ , AND  
THE TEMPERATURE COEFFICIENTS FOR MIC DIELECTRIC  
RESONATOR STRUCTURES

$L_1/h$	$\epsilon_{rs}$	$f/f_{\text{rod}}$	$p_e^{-1}$	$A$	$C_d$	$C_m$	$C_{L_1}$	$\tau_{\epsilon_r}$	$\tau_{\epsilon_{rs}}$
0.06	1.0	0.9677	1.004	130.0	-4384	-5637	+.0024	-4978	-0.0002
	2.5	0.9677	1.004	130.0	-4384	-5636	+.0024	-4978	-0.0005
	10.0	0.9676	1.004	130.0	-4384	-5632	+.0016	-4976	-0.0019
	8	0.8254	1.024	316.4	-9742	-0.0052	-0.0206	-4883	-0.0001
	2.5	0.8251	1.024	316.3	-9742	-0.0052	-0.0206	-4883	-0.0002
	10.0	0.8250	1.024	315.5	-9740	-0.0052	-0.0208	-4883	-0.0004
0.24	1.0	0.9057	1.007	180.5	-4920	-5556	+.0477	-4965	-0.0035
	2.5	0.9049	1.009	179.3	-4920	-5556	+.0456	-4958	-0.0140
	10.0	0.9010	1.018	173.1	-4915	-5431	+.0346	-4911	-0.0603
	8	0.7851	1.025	525.6	-9448	-0.0075	-0.0477	-4878	-0.0033
	2.5	0.7847	1.026	517.0	-9437	-0.0075	-0.0488	-4873	-0.0085
	10.0	0.7827	1.032	476.0	-9379	-0.0076	-0.0545	-4845	-0.0357

$\epsilon_r = 35$ ,  $a/h = 1.00$ ,  $b = \infty$ . The results have been obtained by means of the modified Rayleigh-Ritz method with  $N = 25$ .

is smaller than 0.4 percent and smaller than 0.15 percent of frequency values.

As the next example, we consider open-type DR's on a dielectric substrate. The results of computations using the modified Rayleigh-Ritz method are shown in Table V. We note that for small thickness of the substrate ( $L_1 = 0.06h$ ) its permittivity has a negligible influence on the resonant  $TE_{018}$ -mode frequency of the system. Even for relatively thick substrates ( $L_1 = 0.24h$ ) the influence of  $\epsilon_{rs}$  on the frequency value is not greater than 0.5 percent for the DR structures considered in Table V. Now we consider the problem of thermal stabilization of the resonant frequency for different DR systems. Using the numerical results presented in Tables I-V and equations (8)-(10) we can determine all the coefficients required for the calculation, assuming that material properties are known. It is seen from the results presented in Tables III and IV that for  $\epsilon_r = 35$  and  $a/h \geq 0.5$  the  $C_m$  coefficient values are smaller than 0.01 if the distance  $L$  and radius  $b$  are sufficiently large. Assuming that  $\alpha_m \leq 25 \text{ ppm}/^\circ\text{C}$  (as occurs for all metals used in practice), the influence of thermal expansion of the metal shield on  $\tau_f$  is smaller than 0.25  $\text{ppm}/^\circ\text{C}$  in such cases. Such systems are useful for measurements of  $\tau_{\epsilon_r}$  coefficients if the  $\alpha_d$  coefficient is known. For a cavity almost completely filled with a dielectric, the values of  $C_m$  and  $C_d$  are  $C_m \approx -1$  and  $C_d \approx 0$ . Theoretically such systems can also be useful for measurements if the  $\alpha_m$  value is known. Since the  $C_m$  and  $C_d$  coefficients change their values with the distance  $L$ , it is difficult in practice to get thermally stable tunable DR systems. Theoretically it is possible to get  $\tau_f = 0$  for tunable systems if  $L_1/h \approx 0$ ,  $\alpha_m = \alpha_d$ , and  $\tau_{\epsilon_r} = -2\alpha_d$ , assuming that the mode of interest is interior ( $p_e \approx 1$ ).

As the last example we consider  $TE_{018}$ -mode resonant systems whose substrate is made of material having any value of the imaginary part of permittivity  $\text{Im}(\epsilon_{rs})$ . Complex frequency mode-matching method has been used for computations [4]. The results of computations are shown in Fig. 6. Maximum value of  $\text{Im}(\epsilon_{rs}) \approx 10^8$  corresponds approximately to silver conductivity. We can notice that for  $\text{Im}(\epsilon_{rs}) > 10^4$  the substrate can be considered as made of metal (more precisely, the substrate can be treated as made of metal if its thickness is many times greater than the depth of penetration for particular  $\text{Im}(\epsilon_{rs})$  and frequency values). For such values of  $\text{Im}(\epsilon_{rs})$  one can use the approximate methods of the resonant frequency and  $Q_u$ -factor computations (the same as described for low-loss systems). The approximate methods can also be used for computations if  $\text{Im}(\epsilon_{rs})$  values are

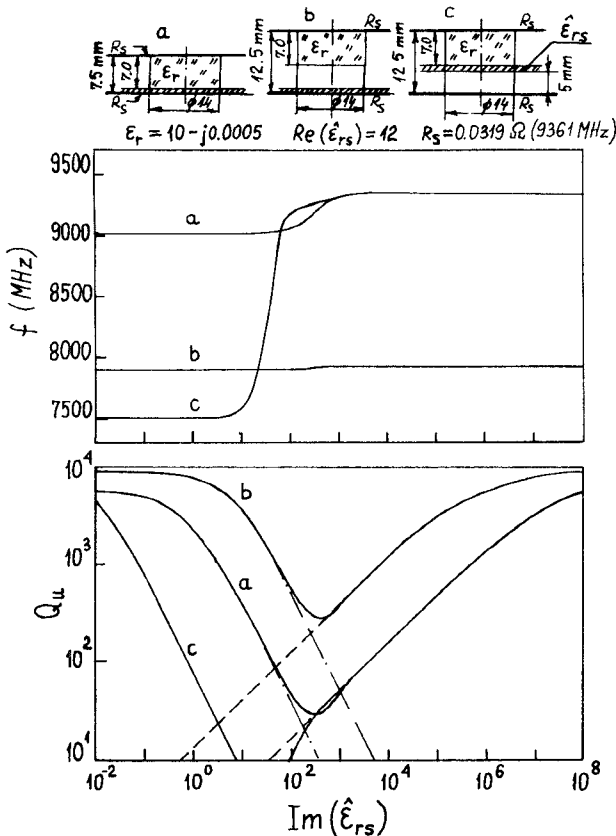


Fig. 6.  $TE_{01s}$ -mode frequencies and unloaded  $Q_u$ -factor values versus the imaginary part of substrate permittivity  $Im(\epsilon_{rs})$ . The results have been obtained by means of the complex mode-matching method with  $N=5$ . Dashed lines indicate  $Q_u$ -factor values computed by means of perturbation theory with real mode-matching method.

small. For the systems considered in Fig. 6, a small  $Im(\epsilon_{rs})$  value means any value smaller than 1. As is seen, only in relatively narrow ranges of  $Im(\epsilon_{rs})$  must complex frequency formalism be used for the resonant frequency and  $Q_u$ -factor computations.

#### REFERENCES

- [1] U. Crombach and R. Michelfeit, "Rezonanzfrequenzen und Feldstärken in geschirmten dielektrischen Sheiben und Ringresonatoren," *Frequenz*, vol. 35, no. 12, pp. 324-328, 1981.
- [2] Y. Kobayashi, N. Fukuoka, and S. Yoshida, "Resonant modes for a shielded dielectric rod resonator," *Electronics and Communication in Japan*, vol. 64-B, no. 11, pp. 46-51, 1981.
- [3] Y. Kobayashi, T. Aoki, and Y. Kabe, "Influence of conductor shields on the  $Q$ -factors of a  $TE_0$  dielectric resonator," in *IEEE MTT-S Int. Microwave Symp. Dig.* (St. Louis), June 1985, pp. 281-284.
- [4] J. Krupka and Sz. Maj, "Application of  $TE_{01s}$  mode dielectric resonator for the complex permittivity measurements of semiconductors," in *CPFM'86 Conf. Dig.* (Gaithersburg), June 23-27, 1986, pp. 154-155.
- [5] F. H. Gil and J. Gisermo, "Finite element analysis of dielectric resonators on microstrip structures," in *Proc. XXIst General Assembly of URSI* (Florence, Italy), Aug. 28-Sept. 5, 1984.
- [6] P. S. Kooi, M. S. Leong, and A. L. S. Prakash, "Finite element analysis of the shielded cylindrical dielectric resonator," *Proc. Inst. Elec. Eng.*, pt. H, vol. 132, pp. 7-16, Feb. 1985.
- [7] J. Delaballe, P. Guillon, and Y. Garault, "Local complex permittivity measurement on MIC substrates," *Arch. Elek. Übertragung*, vol. 35, no. 2, pp. 80-83, 1981.
- [8] J. Krupka, "Optimization of an electrodynamic basis for determination of the resonant frequencies of microwave cavities partially filled with a dielectric," *IEEE Trans. Microwave Theory Tech.*, vol. MTT-31, pp. 302-305, Mar. 1983.

- [9] J. Krupka, "Computations of frequencies and intrinsic  $Q$ -factors of  $TE_{0nm}$  modes of dielectric resonators," *IEEE Trans. Microwave Theory Tech.*, vol. MTT-33, pp. 274-277, Mar. 1985.
- [10] D. Kajfez and P. Guillon, *Dielectric Resonators*. Dedham, MA: Artech House, 1986, ch. 7.
- [11] D. Kajfez, "Incremental frequency rule for computing the  $Q$ -factor of a shielded  $TE_{0mp}$  dielectric resonator," *IEEE Trans. Microwave Theory Tech.*, vol. MTT-32, pp. 941-943, Aug. 1984.
- [12] N. Imai and K. Yamamoto, "A design of high- $Q$  dielectric resonators for MIC applications," *Electronics and Communications in Japan*, vol. 67-B, pp. 59-67, Dec. 1984.

#### Composite Inductive Posts in Waveguide— A Multifilament Analysis

GAD S. SHEAFFER, MEMBER, IEEE, AND  
YEHUDA LEVIATAN, MEMBER, IEEE

**Abstract**—A multifilament moment solution for the analysis of composite dielectric posts in rectangular waveguide is presented. This method permits the analysis of inductive posts composed of disparate regions, each with its own homogeneous complex permittivity. The solution uses the fields generated by sets of fixed-amplitude current filaments to simulate both the field scattered by the posts and the field inside every homogeneous region comprising the posts. Point matching the electric and magnetic fields on the boundaries between regions of different permittivity yields the as yet unknown amplitudes for the current filaments. These currents can in turn be used to calculate field-related parameters of interest such as the scattering matrix and the equivalent circuit parameters. Inductive posts of any shape, composition, size, location, and number can be handled by this method accurately and with very good numerical efficiency. The results obtained are in good agreement with the few cases for which data are available. They also behave well in the limiting cases studied. The solution is further applied to other situations for which no experimental or calculated results are known.

#### I. INTRODUCTION

The study of dielectric waveguide posts of the inductive type is gaining momentum, with a number of works published. In a recent work by the authors [1], a rapidly converging moment solution for the analysis of homogeneous dielectric posts of the inductive type in rectangular waveguide has been suggested. The solution in [1] is numerically efficient and general in that inductive posts of arbitrary smooth shape, size, location, and number can be handled. It is, however, restricted to homogeneous posts and, furthermore, the formulation introduced there deals explicitly with a single post.

A list of useful references to a large body of work on homogeneous dielectric posts can be found in [1]. Composite posts, that is, posts homogeneous only in parts, have received much less attention. Perhaps the only analysis of anything that can be classified as a composite post problem is the work initiated by Nielsen [2] and pursued by Gotsis, Vafiadis, and Sahalos [3]. In these works, a circular post composed of two concentric regions, each with its own permittivity, was analyzed with the goal of

Manuscript received September 16, 1987; revised November 28, 1987.

G. S. Sheaffer is with OPTOMIC Technologies Corporation Ltd., Science-Based Industrial Park, Technion City, Haifa 32000, Israel.

Y. Leviatan is with the Department of Electrical Engineering, Technion—Israel Institute of Technology, Haifa 32000, Israel.

IEEE Log Number 8719441.